Structure and Cooperativity of a T-State Mutant of Histidine Decarboxylase From *Lactobacillus* 30a

Scott Worley, Elisabeth Schelp, Arthur F. Monzingo, Stephen Ernst, and Jon D. Robertus[*]
Institute of Cellular and Molecular Biology, Department of Chemistry and Biochemistry, University of Texas, Austin Texas

ABSTRACT Histidine decarboxylase (HDC) from *Lactobacillus* 30a converts histidine to histamine, a process that enables the bacteria to maintain the optimum pH range for cell growth. HDC is regulated by pH; it is active at low pH and inactive at neutral to alkaline pH. The X-ray structure of HDC at pH 8 revealed that a helix was disordered, resulting in the disruption of the substrate-binding site. The HDC trimer has also been shown to exhibit cooperative kinetics at neutral pH, that is, histidine can trigger a T-state to R-state transition. The D53,54N mutant of HDC has an elevated Km, even at low pH, indicating that the enzyme assumes the low activity T-state. We have solved the structures of the D53,54N mutant at low pH, with and without the substrate analog histidine methyl ester (HME) bound. Structural analysis shows that the apo-D53,54N mutant is in the inactive or T-state and that binding of the substrate analog induces the enzyme to adopt the active or R-state. A mechanism for the cooperative transition is proposed. Proteins 2002; 46:321–329. © 2002 Wiley-Liss, Inc.

Key words: histidine decarboxylase; helix disorder; enzyme activation; mutation; cooperativity

INTRODUCTION

Lactobacillus 30a are lactic acid-producing bacteria. As they metabolize, their secretion of acid can reduce the environmental pH to about 4, where growth stops. To counter this effect, the bacteria secrete histamine base. The secretion of histamine is part of a histidine-histamine antiport mechanism that can also be used to generate ATP.[1] Histamine is the product of histidine decarboxylase (HDC), and the activity of this enzyme allows denser growth than is seen for mutant strains lacking HDC.[2] HDC activity is pH dependent. The enzyme is inactive at neutral and alkaline pH and is activated at acidic conditions.

The biochemical properties of HDC from *L.* 30a have been thoroughly studied and reviewed.[3] HDC uses a covalently bound pyruvoyl moiety as a cofactor in the decarboxylation reaction. This cofactor arises from a serinolysis reaction in which a 310-residue proenzyme is cleaved to produce an 81-residue β-chain and a 228-residue α-chain with the pyruvoyl group at its amino terminus.[4] Active HDC, at pH 4.8, has been analyzed at 2.5 Å resolution.[5,6] The enzyme forms a cup-shaped trimer

with a deep central cavity containing three active sites. Each active site is formed at the interface of two HDC monomers. The structure of wild-type HDC complexed with the substrate-analog inhibitor histidine methyl ester (HME) has also been solved.[7]

The enzyme is known to exhibit cooperative, sigmoidal kinetics at neutral pH.[8] The most common models of cooperative kinetics assume an oligomeric protein possessing at least two tertiary and quaternary forms, a low activity Tense (T), and a fully active Relaxed (R) state. We carried out a detailed kinetic analysis of wild-type HDC at pH 7.6 showing that the apparent K_m values for these T and R states were 50 mM and 5 mM, respectively.[9] We recently solved the X-ray structure of wild-type HDC at pH 8, that is, in the T state.[10] The analysis revealed that HDC inhibition at neutral to alkaline pH results from the disordering of helix B that disrupts the substrate-binding site.

We also carried out a program of site-directed mutagenesis to analyze the mechanism and regulation of HDC.[9,11–13] It was observed that mutation of D53 led to an increased K_m, even though the residue is not at the active site. It was proposed that D53 is part of a mechanism controlling the transition between active and inactive states. Some mutants, such as D53N and D53,198N, showed sigmoidal kinetics at pH 4.8, indicating a fairly easy transition from T to R triggered by substrate. Other mutants were more strongly stabilized in the T state, such as the double mutant, D53,54N, in which Asp 53 and Asp 54 were converted to asparagines.[13] In this article we describe the X-ray structures of the apo-D53,54N mutant and its complex with HME at room temperature and at −170°C. A mechanism for cooperativity is also described and is discussed in light of kinetic data for D53,54N and related mutants.

MATERIALS AND METHODS

The D53,54N mutant protein was isolated as described previously for wild-type HDC from *Escherichia coli* cells transformed with a plasmid containing the D53,54N mu-

TABLE I. Crystallographic Data for the D53,54N Mutant of HDC

Space group: C222₁	Room temperature		−170°C	
	HDC	HDC · HME	HDC	HDC · HME
Cell parameters (a,b,c)	98.3, 119.0, 203.8	97.0, 117.8, 205.8	96.2, 115.3, 202.4	96.3, 115.5, 206.4
Resolution (Å)	3.1	3.2	2.6	2.5
R_{merge} (%)	7.9	10.3	8.9	7.3
R_{merge} (last shell) (%)	41.4	45.4	38.9	33.6
I/σ	11.8	10.7	14.1	19.1
I/σ (last shell)	3.6	2.1	2.4	2.7
Completeness (%)	81.8	80.7	97.0	91.4
Unique reflections	17,480	15,945	34,308	39,581
Redundancy	3.3	1.8	2.7	2.9
$R_{working}$	0.270	0.204	0.266	0.243
R_{free}	0.330	0.269	0.317	0.279
RMS deviation				
From ideality				
Bonds (Å)	0.016	0.015	0.017	0.013
Angles (Å)	3.42	2.42	3.40	2.30
RMS Cα distance from	0.99	0.44	0.58	0.45
pH 4.8 wild-type (Å)				

tant gene.[13,14] Crystals were grown at room temperature by the hanging drop vapor diffusion method; drops contained 5 µL of purified histidine decarboxylase (12 mg/mL) and 5 µL of precipitant solution from the well (0–15% PEG₄₀₀, 4–8% PEG₄₀₀₀, 0.1 M sodium acetate, pH 4.6). Crystals containing the protein complexed with HME were formed by soaking in an artificial mother liquor (25% PEG₄₀₀, 0.1 M sodium acetate, pH 4.6) containing 4 mM HME (Sigma Chemical Co., St. Louis, MO) for 24 h.

For low-temperature data collection, crystals were transferred to a cryoloop and were flash frozen by dipping in liquid nitrogen, either immediately or after being dragged through a cryoprotectant solution (25% PEG₄₀₀, 0.1 M sodium acetate, pH 4.6). Frozen crystals were then placed in the coldstream on the goniostat. Cryoloops and the CrystalCap Magnetic System from Hampton Research (Laguna Niguel, CA) were used. X-ray diffraction data were collected at room temperature or at −170°C by using an MSC low-temperature system, an RAXIS IV image plate detector, and a Rigaku rotating anode X-ray generator operating at 50 KV and 100 mA. The diffraction data were processed and reduced with the programs DENZO and SCALEPACK.[15]

Molecular replacement (MR) methods were used to phase the data. The model used was the trimer from the structure of wild-type HDC at pH 4.8[6]; rotation and translation searches and Patterson correlation refinement were performed by using X-PLOR.[16] Before refinement, 10% of the reflections were set aside for cross-validation.[17] Rigid body refinement of the trimer, and of each monomer, was performed by using X-PLOR. The resulting models were refined by using the slow cooling protocol of X-PLOR. To facilitate manual rebuilding of the model, difference maps and 2Fo-Fc maps, weighted by LBEST[18] or by the SIGMAA method,[19] were prepared. Omit maps of the form $(F_o-F_c)\alpha_{calc}$ were also calculated by using X-PLOR. Further refinement was performed by using REFMAC.[20] For the final stages of refinement, a bulk solvent correction was applied to the model-calculated structure factors using X-PLOR. Model building was carried out on a Silicon Graphics Indy computer using O.[21] MAPMAN[22] was used to help position bound solvent molecules. The refined structures were analyzed by using PROCHECK.[23]

Atomic Coordinates

Coordinates of the four refined models have been deposited in the Protein Data Bank with entry codes 1IBU, 1IBW, 1IBT, and 1IBV, corresponding, respectively, to the structures listed in columns 2–5 of Table I.

RESULTS AND DISCUSSION

Wild-type HDC crystallizes at pH 4.8 in space group I4₁22 with the asymmetric unit being a trimer of 310 amino acid monomers.[5,24] The D53,54N mutant crystallizes at pH 4.6 in space group C222₁ with the asymmetric unit again being the trimer. Table I shows the crystallographic data summary for the four crystals of D53,54N reported here, each solved independently by molecular replacement methods. Diffraction data collected at −170°C are clearly of higher quality than that collected at room temperature. However, room temperature crystals gave reasonable diffraction to around 3.2 Å and allowed key features of the structure to be seen. The basic HDC model was easy to fit to the electron density in all four cases. Ramachandran plots for the four refined models show that only Gln 22 and Asn 69 are in the disallowed region. These residues are also in the disallowed region in the pH 4.8 wild-type structure, suggesting that they are truly in a strained conformation.

The overall fold of the HDC mutant monomer is essentially identical to that seen previously for the wild-type protein at pH 4.8[6] and at pH 8.[10] The root-mean-square deviations (RMSDs) among visible Cαs for each mutant model compared with the wild-type HDC are shown in Table I. These values, calculated for the entire trimer, show that the quaternary structure is conserved between
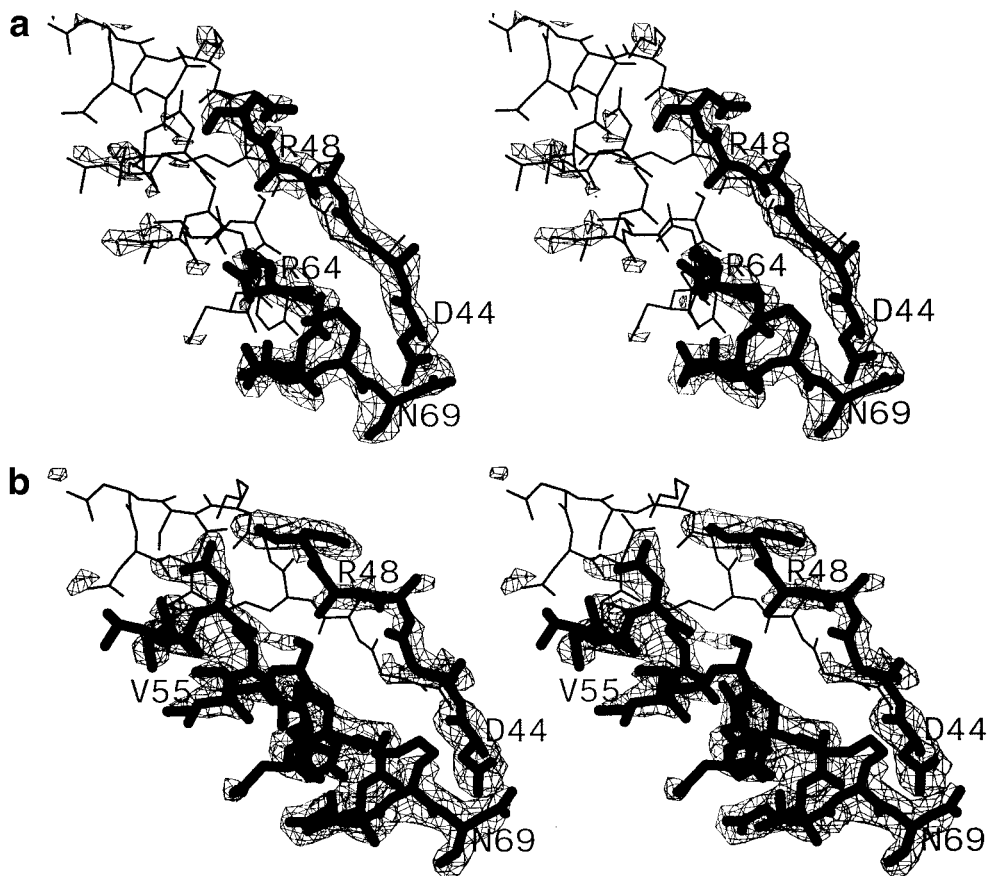
Fig. 1. Electron density for the mutant HDC structures. Electron density for residues 44–69 is shown. The map was calculated with SIGMAA-weighted 2Fo-Fc amplitudes and phases. The electron density basket is contoured at 0.9 σ. The corresponding model is shown in dark bonds. **a:** Density for the room temperature apo-D53,54N crystal and (**b**) the same region from data collected at −170°C. Residues from the least-squares superimposed pH 4.8 wild-type structure are shown in light bonds. **c:** Density for the room temperature D53,54N-HME complex crystal and (**d**) the same region from data collected at −170°C.

the mutant and wild-type enzymes. The mutant trimers do not expand or contract radially from the molecular three-fold axis, nor do the subunits shear with respect to one another.

Structure of Apo-D53,54N Mutant of HDC

The structure of the apo-D53,54N mutant of HDC was determined independently from diffraction data collected at both room temperature (RT) and −170°C. With both structures, the overall fold is similar to the wild type except for residues in the stretch 49–63. Residues 49–63 were also observed to be disordered in the pH 8 wild-type structure.[10] The RMSDs of observed α-carbon positions between the apo-D53,54N structures and the pH 8 structure is around 0.5 Å.

In the RT structure, residues 49–63 are generally disordered and cannot be fit well to electron density, although for any monomer of the trimer, a few of the residues on either end of the range could have been fit and included in the model. Figure 1 shows electron density and the model for a section of HDC from residues 44–69, which includes the 49–63 segment that can change from an

ordered structure to a disordered one. Figure 1(a) shows the region for the apo-D53,54N mutant at RT and indicates that the region is largely disordered. In particular, there is no significant density for residues 50–63.

In the cryo-cooled structure, more residues of the 49–63 region appeared to be ordered and could be fit, although the degree of order varies with each monomer. In all three monomers, the upper part of helix B (residues 55–63) is ordered. The backbone, but not all of the side-chains, of the loop preceding the helix (residues 49–54) could be fit in two of the monomers. In one of the monomers, the region appears to be very similar to the wild-type pH 4.8 (R-state) structure, with an RMSD of 1.0 Å for Cαs of this stretch. In another monomer, the loop can be traced but is less like the wild type with an RMSD of 2.5 Å. Finally, this same loop appears to be completely disordered in the third monomer, for which electron density is shown in Figure 1(b).

In summary, the disorder seen in region 49–63 of the mutant resembles that seen for the wild type at pH 8. This structural data, coupled with kinetic data, indicate that the low activity T state of HDC is represented by
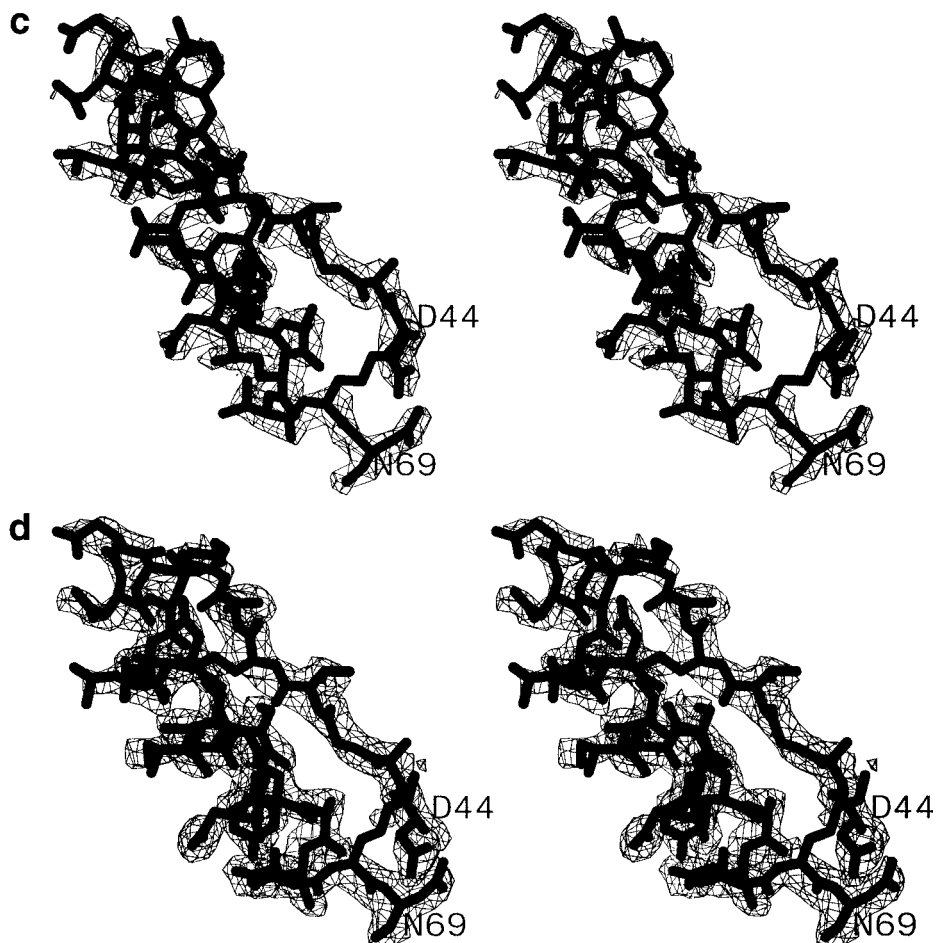
Figure 1.   (Continued.)

both the pH 8 structure and the D53,54N structure at pH 4.6.

Structure of D53,54N Mutant Complexed With HME

HME is identical to the substrate of HDC, histidine, except that the carboxylate group has been converted to the methyl ester. Like histidine, HME is known to form a Schiff base with the pyruvoyl moiety of the enzyme.[25] However, the methyl ester makes decarboxylation impossible, and as a result, the enzyme is irreversibly inactivated.[26] The structure of the wild-type enzyme complexed with HME at pH 4.8 was previously described.[7]

Like the wild-type enzyme, D53,54N is completely inactivated by HME. We assume the resulting structure should resemble that of the mutant enzyme at extremely high substrate concentration, that is, the inhibited enzyme should assume the R state. The structure of the D53,54N mutant complexed with the substrate analog inhibitor HME was determined from data collected at both RT and −170°C. Both of these structures are very similar to the wild-type R structure with an RMSD in Cα position of 0.5 Å. Unlike the apo form of the double mutant, residues 49–63 are ordered in the complex and resemble the wild-type R structure [Fig. 1(c,d)].

Electron density for HME in the complex was clear, and in the same position observed for the inhibitor in the wild-type protein at pH 4.8.[7] The interactions are shown in Figure 2. The side-chain of Y62, disordered in the apoenzyme, is oriented so that its hydroxyl group forms a hydrogen bond with the carboxyl of terminal S81, as reported previously with the binding of HME to the wild-type protein. Ile 59 is also ordered by interaction with HME and forms the top of the imidazole-binding site. These two residues were observed to undergo the largest conformational change when a complex is formed with the wild-type enzyme. It appears that they are a very important for substrate recognition and make energetically favorable contacts that help define the productive active site geometry.

Additional hydrogen bonds are formed with the carboxylate group of E197 and with the carbonyl oxygen of F195. As with the wild-type enzyme, a hydrogen bond between the amide nitrogen of F195 and the carbonyl oxygen of the pyruvoyl moiety is also observed. The similarity of the complex structure to the pH 4.8 wild-type structure indicates that the binding of a substrate analog (and presumably substrate) to the mutant protein induces it to take the R-state conformation.
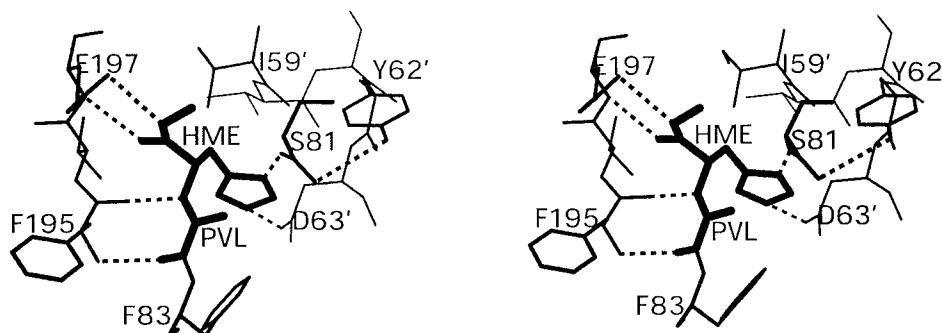
Fig. 2. Binding of HME in the active site of the D53,54N mutant of HDC. Residues from the right-hand monomer of the molecular interface are labeled with (′). The pyruvoyl moiety (PVL) is part of the left-hand monomer and is shown bonded to HME. Hydrogen bonds are drawn with dashed lines. This figure was made by using MOLSCRIPT.[28]

Role of Residues 49–63 in Control of HDC Activity

We recently compared the structure of wild-type HDC in the fully active R state (pH 4.8) and the low activity T state (pH 8); we found the main difference to be a transition of residues 49–63 from an ordered to a disordered state.[10] In this article we examined the structure of an apoenzyme double mutant of HDC (D53,54N), which is known from kinetics analysis to assume the T state, even at pH 4.8. Again, the main finding is that this region of the protein is disordered. This malleable segment lies on the surface of the enzyme, at the interface with another monomer. The active site is composed of residues from both molecules of the interface, and the C-terminal end of the flexible segment contributes strongly to the substrate-binding site. In particular, D63′ forms an ion pair with the substrate imidazolium, whereas Y62′ and I59′ move in to create the substrate-binding pocket. When this segment is disordered, it is difficult to bind substrate. This can be seen by examining the K_m for various proteins. At pH 4.8 the R form (wild type) has a K_m of 0.2 mM, whereas the T state (D53,54N) has a K_m of 9.8 mM.[13] At pH 7.6, deprotonation of the substrate imidazolium makes the substrate harder to bind, but a Hill plot analysis shows that the R state has a 10-fold lower K_m than the T state.[9]

D53′ and D54′ are not at the active site and do not engage the substrate directly. The structural effects of the mutations at positions 53 and 54 were more extensive than might be expected for typical point mutants. At pH 4.6 and room temperature, the mutant protein exhibited a disordering similar to that of the wild-type enzyme at pH 8. There was no interpretable electron density corresponding to residues 49–63, and the protein is disordered or in high thermal motion in this region. Clearly, the free energy differences between the R and T states are small, and the equilibrium can be shifted by the mutations. At this pH, wild-type HDC is well ordered in this area and shows that D198 from one monomer forms a pair of short hydrogen bonds with D53′ across the molecular interface. This can only occur if the two carboxylates are protonated and electrostatically neutralized at low pH. The mutant apparently cannot form this kind of interaction, although it is reasonable to assume that the asparagine group at position 53′ could hydrogen bond with D198. Apparently, the hydrogen bonding possible for the mutant is weaker than that between two protonated acids and cannot stabilize the R state at room temperature.

The binding of HME to the D53,54N mutant mimics the effect of very high substrate concentrations; it induces residues 49–63 to form a conformation very similar to that observed in the wild-type R-state protein at pH 4.8. In the wild-type protein, the carboxylate group of D53′ forms hydrogen bonds with the carboxylate group of D198. This interaction has been referred to as a "proton trap."[13] In the mutant-HME complex, the side-chain of N53′ is rotated so that the amide group can form potential hydrogen bonds with the side-chains of R48′, S51′, D52′, and R217. The carboxylate group of Asp 198 appears to form a salt link with Arg 217. The side-chain of 54′ interacts with the side-chain of K50′ in both the wild-type and mutant-HME complex structures, apparently forming a link between the end of strand 3 and the beginning of helix B and stabilizing the β-turn-α structure. The structure is further stabilized by potential salt links of R48′ and K50′ (on strand 3) with D57′ (on helix B). Also stabilizing the induced conformation are salt links across the molecular interface of R48′ and R64′ with E227. These same interactions are observed in the pH 4.8 wild-type structure, but neither is observed in the apo-mutant structure nor in the pH 8 structure.

Binding HME to the D53,54N enzyme triggers a conformational change that organizes the active site residues of helix B. A hydrogen bond is formed between the carboxylate side-chain of D63′ (on helix B) and the NE2 atom of HME. In addition, Y62′ and I59′ (both on helix B) become ordered and form the HME-binding pocket. Kinetic data from site-directed mutants have shown these residues to be important in substrate binding. The D63N mutant shows a 200-fold increase in K_m compared with wild-type at pH 4.8.[9] The I59A mutant is completely inactive, whereas the I59V mutant has a K_m comparable to wild-type at pH 4.8.

At −170°C, the 49–63 segment of the apo-D53,54N protein is somewhat more ordered than that observed at room temperature, with the backbone of one of the monomers being nearly identical to the wild type. However,

even though more of the main chain is observed to be more ordered than at room temperature, many of the side-chains, including key side-chains such as R48 and N54, are disordered. This finding indicates that the ordering is induced by the low temperature rather than the stabilizing side-chain interactions observed in the wild-type and HME-D53,54N structures. The variability of backbone structure suggests that this region is in thermal motion, even under cryo-cooled conditions.

β-Sandwich and Helix C Movement

One of the more distinctive structural features of the HDC monomer is a prominent β-sandwich, which primarily consists of two face-to-face three-strand antiparallel sheets, previously labeled sheets II and III.[6] Aside from the disorder/order of helix B and its preceding loop (residues 49–63), another prominent difference in structure between the R and T structures is a small, but significant, movement of the β-sandwich and helix C. This movement is seen when comparing the wild-type enzyme at pH 4.8 and pH 8, and when comparing the apo and HME complexed forms of the D53,54N mutant enzyme. Sheet II is primarily composed of strands 3, 11 (residues 148–161), and strand 15 (residues 251–265). Strands 12 (residues 174–184), 13 (residues 193–202), and 14 (residues 238–248) mainly form sheet III. Helix C returns strand 13 to strand 14 in sheet III.

This conformational difference between T- and R-state structures is shown in Figure 3. In Figure 3(a), the RT apo-D53,54N and D53,54N-HME structures are superimposed, whereas the wild-type pH 8 and pH 4.8 structures are superimposed in Figure 3(b). The transition can be characterized by a 10° rotation of the upper sections of the three strands of sheet II and strands 12 and 13 of sheet III about an axis virtually parallel to the sheets, and an independent rotation of 6° of helix C about an axis normal to the direction of the helix. Essentially, the rotation in the β-sandwich pulls on helix C, causing it to rotate. When structures are superimposed by using the Cα positions, which precede and follow the β-sandwich in the primary sequence (residues 1–37 and 264–310), the RMSD of the β-sandwich and helix C between the apo- and complexed mutant structures is 1.0 Å. A similar superposition of the pH 8 and pH 4.8 wild-type structures also yields an RMSD of 1.0 Å. However, some distances are larger. For example, the distance between the E227 Cα positions of R- and T-state structures is 2.1 Å. By contrast, the RMSD of the β-sandwich and helix C between apo-D53,54N and pH 8 wild-type (T-state) structures is 0.5 Å and between D53,54N-HME and pH 4.8 wild-type (R-state) structures is 0.4 Å.

Strand 3 (residues 38–50) of sheet II is partially disordered in the T-state structures as has been described above. In fact, the RMS distance of the observed Cα positions of this strand compared with those of the pH 4.8 wild-type structure is around 2 Å. The hydrogen-bonding pattern with the adjacent β-strand of the sheet is maintained, however, so that conformational changes are transmitted through the sheet. Hydrogen bonds between strand 11 of sheet II and strand 12 of sheet III facilitate the propagation of the change to sheet III. The movement is propagated through sheet III to strand 13, which contains key residues E197 and D198. E197 acts as an acid in the HDC mechanism, based on its structural position[7] and the kinetic analysis of site-directed mutants.[11] D198 is known to hydrogen bond across the molecular interface to D53′ in the wild-type R structure. Finally, the conformational change of strand 13 is propagated to the adjoining helix C, which contains residues R217 and E227. These residues also participate in ion pairs across the molecular interface in the R-state structures.

A Possible Mechanism of Cooperativity

Kinetic data show that HDC is essentially inactive at neutral and alkaline pH and active at low pH. That is, low pH shifts HDC from the inactive (T) state to the active (R) state. This pH-induced alteration is physiologically relevant to the control of HDC activity because it is advantageous for the cells to generate histamine to counteract the local effects of lactic acid production. It is not clear if the pH-induced conversion of HDC from the T to the R state is mechanically cooperative. That is, we do not know if protonation of one active site "trap" induces an ordering that is transmitted mechanically to other HDC sites and helps to order them. It is plausible that this happens, but it may also be that protonation occurs almost simultaneously at all sites so that a given HDC trimer is effectively all in the R or all in the T state, depending on pH.

It has been observed at pH 7.6 that HDC exhibits sigmoidal kinetics.[8] At pH 4.8, HDC mutants D53N and D53,198N also show cooperative kinetics with a Hill number of 1.6–1.7.[13] This means that histidine can shift the enzyme from the T to the R state and shows that substrate, along with protons, can stabilize the active R state. Furthermore, the kinetics show that histidine stabilization is cooperative and, therefore, must be mechanically transmitted from one site to another. It is not clear how physiologically important substrate-induced cooperativity is. At low pH, protons can fully activate the enzyme, and so substrate concentration has little effect on activity. At pH 7.6, >100 mM substrate is required to activate HDC 50%, and this is not physiologically relevant. Nevertheless, it is still of scientific interest to examine the mechanics of the T to R transition. It may play a subtle role in the pH activation of the enzyme and may also contribute to total HDC activity at intermediate pH values.

We get a static view of the mechanics of cooperativity by comparing the R and T states seen in the wild-type and the D53,54N mutant HDCs (Fig. 3). Major differences are seen in (a) helix B and its preceding loop and (b) the conformational shift of the adjoining β-sandwich and helix C. Just above we described a possible path whereby a conformational change at one site, organization of helix B and movement of strand 3, is transmitted across the molecule via the β-sandwich, to helix C. The movement of helix C may help organize the next active site around the HDC cyclic trimer.
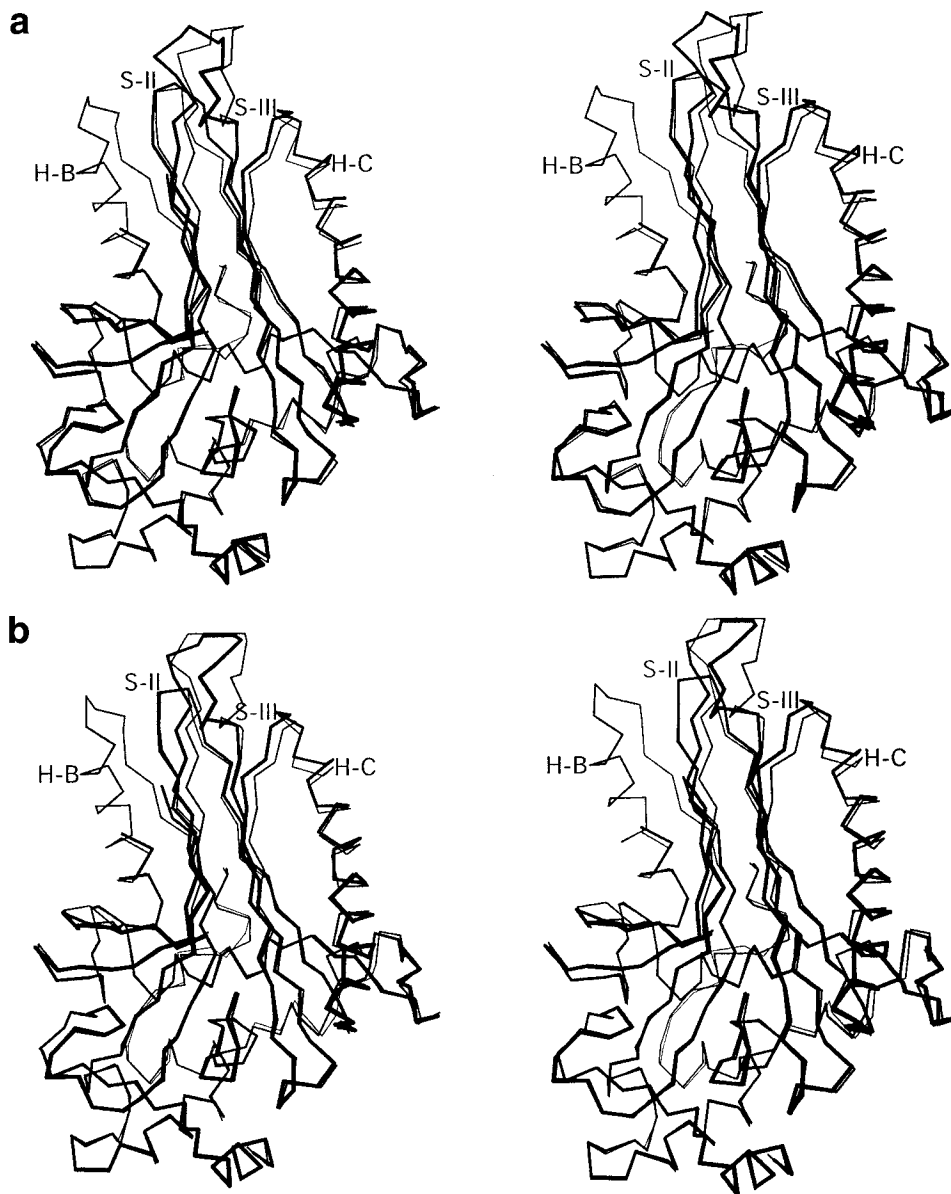
Fig. 3.   Cα superposition of T-state and R-state models. **a:** Cα superposition of the RT apo-D53,54N (T-state) and D53,54N-HME (R-state) models. **b:** Cα superposition of the wild-type pH 8 (T-state) and pH 4.8 (R-state) models. In both panels, the T-state model is shown with dark bonds and R-state model with light bonds. The structures were superimposed by using the Cα positions, which precede and follow the β-sandwich in the primary sequence (residues 1–37 and 264–310). The RMSD for these atoms, which lie mostly in the lower part of the figure, is 0.4 Å. The RMSD of the β-sandwich and helix C between the R- and T-state structures is 1.0 Å. This figure was made by using MOLSCRIPT.[28]

The importance of helix C in forming interactions across the molecular interface is most clearly shown by the interaction of E227 (on helix C of one monomer) with R64′ (on helix B′ of an adjacent monomer), as shown in Figure 4. In the R-state structures, the inter-Cα distance between E227 and R64′ is ≈9 Å, and a salt link is formed between the carboxylate and guanidinium side-chains. However, in the T-state structures, the same inter-Cα distance is ≈12 Å, and no salt link is formed. It is of interest that residue 64 is the first ordered residue in helix B in the T-state structures.

In addition, another salt link across the molecular interface is observed in the R-state structures between R217 (on the upper section of helix C) and D52′ (at the beginning of helix B′). D52′ is disordered in the T-state structures. Thus, there are two salt links across the molecular interface observed in the R state, which are absent in the T state. Salt links also play an important role in the cooperative transition of hemoglobin.[27] For example, in the T (deoxy) state of hemoglobin, H146 of the β-chain forms an ion pair with D94, which helps stabilize the T state. H146 loses a proton at higher pH, disrupting
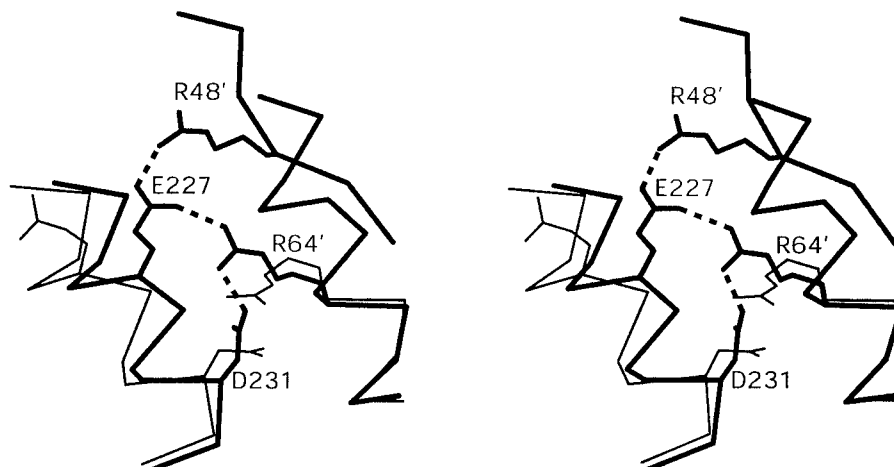
Fig. 4.   Superposition of the wild-type pH 8 (T-state) and pH 4.8 (R-state) models at the molecular interface shows how the change in the position of residue E227 affects its interaction with R64′. The pH 8 model is shown with light bonds and pH 4.8 model with dark bonds. In the R-state model, E227 forms ion pair interactions across the molecular interface with R48′ and R64′. R64′ also forms an interaction with D231. In the T state, interactions with E227 are not observed. R64′ only interacts with D231, and R48′ is disordered. This figure was made by using MOLSCRIPT.[28]

the ion pair, and the structure is driven toward the R (oxy) state.

In summary, we know from kinetics that histidine can trigger a cooperative T to R transition, although the physiological significance of this action is uncertain. The presence of histidine organizes and stabilizes the B helix in the active site. Strand 3 is rearranged in the β-sandwich, and this triggers a subtle adjustment along the sandwich and across the molecule to helix C. Helix C moves closer to the disordered 49–63 segment and stabilizes the ordered configuration through specific ion pairs. This forms an active site structure that can accommodate substrate with a lowered K_m. It may also be that protonation of the D198/D53′ trap organizes a given local active site in a similar fashion and that this information is mechanically transferred, via the β-sandwich, to neighboring sites where a closer juxtaposition of helix C and the potential B helix facilitates that organization as well.

CONCLUSION

The crystal structure of the D53,54N mutant of histidine decarboxylase at low pH reveals a disorganized active site due to the disorder of helix B; this is consistent with its high K_m for substrate binding. This mutant structure is virtually identical to that of the wild-type protein at pH 8, where the enzyme is similarly inactive. Addition of the substrate analog histidine methyl ester induces ordering of helix B and organization of the active site in the D53,54N mutant. The substrate-induced conformation is virtually identical to that of the wild-type protein at low pH, where the enzyme is fully active. This substrate-induced activation is probably similar to that observed for wild-type HDC at neutral to alkaline pH. Binding of histidine methyl ester also causes a slight movement of the β-sandwich and helix C, which may contribute to the cooperative organization of an adjacent active site in the

HDC trimer. Again, this cooperative mechanism is probably similar to that observed for substrate-induced cooperative kinetics of wild-type HDC at neutral to alkaline pH.

REFERENCES

1. Molenaar D, Bosscher JS, Brink B, Driessen AJM, Konings WN. Generation of a proton motive force by histidine decarboxylation and electrogenic histidine/histamine antiport in *Lactobacillus buchneri*. J Bacteriol 1993;175:2864–2870.
2. Recsei PA, Snell EE. Histidine decarboxylase mutants of *Lactobacillus* 30a: isolation and growth properties. J Bacteriol 1972;112:624–626.
3. van Poelje PD, Snell EE. Pyruvoyl-dependent enzymes. Annu Rev Biochem 1990;59:29–59.
4. Recsei PA, Huynh QK, Snell EE. Conversion of prohistidine decarboxylase to histidine decarboxylase: peptide chain cleavage by nonhydrolytic serinolysis. Proc Natl Acad Sci USA 1983;80:973–977.
5. Parks EH, Ernst SR, Hamlin R, Xuong NgH, Hackert, ML. Structure determination of histidine decarboxylase from *Lactobacillus* 30a at 3.0 Å resolution. J Mol Biol 1985;182:455–465.
6. Gallagher T, Rozwarski DA, Ernst SR, Hackert ML. Refined structure of pyruvoyl-dependent histidine decarboxylase from *Lactobacillus* 30a. J Mol Biol 1993;230:516–528.
7. Gallagher T, Snell EE, Hackert ML. Pyruvoyl-dependent histidine decarboxylase: active site structure and mechanistic analysis. J Biol Chem 1989;264:12737–12743.
8. Recsei PA, Snell EE. Histidine decarboxylase of *Lactobacillus* 30a. VI. Mechanism of action and kinetic properties. Biochemistry 1970;9:1492–1497.
9. Pishko EJ, Robertus JD. Site-directed alteration of three active-site residues of a pyruvoyl-dependent histidine decarboxylase. Biochemistry 1993;32:4943–4948.
10. Schelp E, Worley S, Monzingo AF, Ernst S, Robertus JD. pH-induced structural changes regulate histidine decarboxylase activity in *Lactobacillus* 30a. J Mol Biol 2001;306:727–732.
11. McElroy HE, Robertus JD. Site-directed alteration of Glu197 and Glu66 in a pyruvoyl-dependent histidine decarboxylase. Protein Eng 1989;3:43–48.
12. Gelfman CM, Copeland WC, Robertus JD. Site-directed alteration of four active site residues of a pyruvoyl-dependent histidine decarboxylase. Biochemistry 1991;30:1057–1062.
13. Pishko EJ, Potter KA, Robertus JD. Site-directed mutagenesis of intersubunit boundary residues in histidine decarboxylase, a

pH-dependent allosteric enzyme. Biochemistry 1985;34:6069–6073.

14. Copeland WC, Vanderslice P, Robertus JD. Expression and characterization of *Lactobacillus* 30a histidine decarboxylase in *Escherichia coli*. Protein Eng 1987;1:419–423.

15. Otwinowski Z, Minor W. Processing of X-ray diffraction data collected in oscillation mode. Methods Enzymol 1997;27:307–326.

16. Brünger AT. X-PLOR version 3.1: a system for X-ray crystallography and NMR. New Haven: Yale University Press; 1992.

17. Brünger AT. Assessment of phase accuracy by cross validation: the free R value. Acta Crystallogr D 1993;4:129–147.

18. Urzhumtsev AG, Skovoroda TD, Lunin VY. A procedure compatible with X-PLOR for the calculation of electron-density maps weighted using an R-free-likelihood approach. J Appl Crystallogr 1996;2:741–744.

19. Read RJ. Improved Fourier coefficients for maps using phases from partial structures with errors. Acta Crystallogr A 1986;42:140–149.

20. Murshudov GN, Vagin AA, Dodson EJ. Refinement of macromolecular structures by the maximum-likelihood method. Acta Crystallogr D 1997;53:240–255.

21. Jones TA, Zou JY, Cowan SW, Kjeldgaard M. Improved methods for building models in electron density maps and the location of errors in these models. Acta Crystallogr A 1991;47:110–119.

22. Kleywegt GJ, Jones TA. xdlMAPMAN and xdlDATAMAN—programs for reformatting, analysis, and manipulation of biomolecular electron-density maps and reflection data sets. Acta Crystallogr D 1996;5:826–828.

23. Laskowski RA, MacArthur MW, Moss DS, Thornton JM. PROCHECK: a program to check the stereochemical quality of protein structures. J Appl Crystallogr 1993;26:283–291.

24. Hackert ML, Meador WE, Oliver RM, Salmon JB, Recsei PA, Snell EE. Crystallization and subunit structure of histidine decarboxylase from *Lactobacillus* 30a. J Biol Chem 1981;256:687–690.

25. Huynh QK, Snell EE. Pyruvoyl-dependent histidine decarboxylase from *Lactobacillus* 30a. Covalent modifications of aspartic acid 191, lysine 155, and the pyruvoyl group. J Biol Chem 1986;261:4389–4394.

26. Lane RS, Manning JM, Snell EE. Histidine decarboxylase of *Lactobacillus* 30a: inactivation and active site labeling by L-histidine methyl ester. Biochemistry 1976;15:4180–4185.

27. Perutz MF, Kilmartin JV, Nishikura K, Fogg JH, Butler PJ, Rollema HS. Identification of residues contributing to the Bohr effect of human hemoglobin. J Mol Biol 1980;138:649–668.

28. Kraulis PJ. MOLSCRIPT: a program to produce both detailed and schematic plots of protein structure. J Appl Crystallogr 1991;24:946–950.